28th AIAA Applied Aerodynamics Conference
28 June - 1 July 2010, Chicago, Illinois

AIAA 2010-4383

Multi Objective Aerodynamic Shape Optimization of High Speed Train Nose Using Adaptive Surrogate Model

V. V. Vytla* P. G. Huang† and R. C. Penmetsa‡*
Wright State University, Dayton, OH, 45435, USA

The objective of this work is to demonstrate the possibility of using adaptive surrogate models for optimization problems which require expensive computations. A hybrid GA−PSO algorithm is combined with a kriging based surrogate model. The suggested method was used to find the optimum shape of a two dimensional nose shape of a high speed train traveling at 350 Km/hr considering both the induced aerodynamic drag and the generated aerodynamic noise. Since the prediction of aerodynamic drag and aerodynamic noise requires computational fluid dynamic simulations, to limit the number of computer simulations required for optimization, a surrogate model identical to the kriging model was used. The accuracy of the surrogate model is checked using the parameter EIV there by updating the surrogate model whenever necessary. The results show that the combined shape optimization algorithm requires a small number of simulations to identify the optimum shape compared with other methods. The suggested method not only requires a small number of simulations but is also robust. This makes the study on the effect of different weights on the optimum shape feasible without the need for additional simulations. The results show that the nose shape should be slightly short and pointed to get the best aerodynamic performance in terms of induced drag and the nose shape should be slightly long and little bit blunt for the least aerodynamic noise generated. The optimum nose shapes fall between these two shapes based upon the choice of the weights. Regarding the choice of the weights for the given two dimensional test geometry the best compromise would be to choose 50% drag and 50 % noise.

I. Introduction

High Speed trains because of their high efficiency, low maintenance and low pollution are considered as an efficient means of mass transportation. The current high speed train can achieve speeds in excess of 350 km/hr and this speed can have a significant impact on the aerodynamic drag it generates. The issues like the aerodynamic noise, which were not considered to be important when the trains were traveling at low speeds will now become important as the speed of train increases. With the maximum speeds in excess of 350 km/hr the acoustic noise and wind related vibration will become an important issue for design and optimization of the modern trains. It was documented that the critical speed at which aerodynamic noise becomes as strong as the mechanical noise is around 300 km/hr.[1] However the advances in the wheel design reduces the mechanical noise levels generated and thereby reducing the critical speed. Of the many things to be considered, It is important to consider both the induced drag and the aerodynamic noise generated when designing the shape of the train. The goal of this research is to identify the optimal shape that induces the least drag and minimizes the acoustic noise. This type of optimization involves multi-functional constraints requiring a complex search algorithm over multiple design spaces to find a global maximum or minimum. CFD Optimization of a train body can be very expensive and therefore one needs to impose restrictions on the number of functional evaluations that can be performed. This computational efficiency is typically achieved through the use of surrogate models like the response surface model. Response surface based

*Graduate Student, Mechanical and Materials Engineering, Wright State University, and AIAA Student Member
†Professor and Chair, Mechanical and Materials Engineering, Wright State University, and AIAA Associate Fellow
‡Associate Professor, Mechanical and Materials Engineering, Wright State University, and AIAA Senior Member.

design optimization[2,3] helps in reducing the number of actual function evaluations necessary to determine the optimum design configuration.

In this paper, a 2-dimensional shape optimization of a high-speed train is performed by considering two objectives, minimize aerodynamic drag and minimize aerodynamic noise. A response surface based optimization algorithm is implemented and the initial training points necessary for building the surrogate model were selected using Latin Hypercube Sampling (LHS) technique, because of its even distribution of samples in the given design space. One CFD simulation was performed at each of the sample location to determine the drag force. In this research, a response surface modeling technique that is typically referred to as the stochastic process modeling is used. This method was selected because of its ability to reproduce the function values exactly at the sample points unlike traditional least square fit based response surface models that have a residual error associated with every sample location. The stochastic process model introduces an additional term into the regression model that simulates residual at any point in the design space based on its correlation to the residuals at the sampled locations. During an optimization process, the accuracy of the response surface model at any of the evaluation points will be quantified using an Expected Improvement Value (EIV) parameter that gives the overall improvement in the predicted value by adding a simulation at that point.[4,5] Therefore, adding sample points in regions that have high variance will result in higher accuracy improvement in the response surface model. In this research, a threshold will be set to determine if a new CFD simulation is needed to update the existing response surface model during the optimization process. By implementing this algorithm new CFD simulations are added only when the EIV exceeds a preset limit and along the path towards the optimum solution. Hence minimizing the simulation cost and maximizing the contributions of each new simulation to the accuracy of the response surface model. The details about the implementation of the above discussed optimization algorithm are discussed in the following sections.

II. Research Approach

The shape optimization process presented in this paper is divided into two steps, first step is the selection of a robust optimization algorithm and second step is to combine the selected optimization algorithm with adaptive surrogate modeling technique to identify the optimum shape of the train.

II.A. Optimization Algorithms

There are several heuristic optimization algorithms in the literature but the most popular algorithms used extensively in engineering are the Genetic Algorithm (GA)[6] and the Particle Swarm Optimization (PSO). These two methods have their own strengths and weaknesses but a common weakness is the robustness. Since they are both dependent on random initialization of samples the optimum tends to be dependent on this initial set of designs. As an effort to combine the benefits of both the GA and PSO algorithms, Hybrid GA-PSO algorithms have been proposed in literature,[7].[8] Therefore, a hybrid GA-PSO algorithm as shown in Figure 1 is suggested to improve the robustness of the optimization algorithm and it is observed to perform better than or at least as good as either the original GA or PSO algorithms. This algorithm is similar to the one proposed by Settles,[7] but instead of treating the entire population once per generation, we treat it as two halves and use each half to update the local best and global best values which showed improvement of the search process. The details about the proposed algorithm are presented by Vytla[9].

II.B. Response Surface modeling

The use of computer simulations to study and analyze the designs can sometimes be very expensive. This problem becomes more acute during the optimization process when comparing different designs, because of the requirement of large computational resources and the time involved to achieve the result. The cost involved in getting the response for computationally expensive functions like the drag is very high both in terms of computing time and money involved therefore one needs to impose restrictions on the number of functional evaluations that can be performed. Response surface/ surrogate model based design optimization helps in reducing the number of real function evaluations necessary to achieve this goal[2].[3]

The first step in creating the surrogate model is the selection of the parameters for the design variables. With the design space being identified the next step is to identify the design values that will be used to create the surrogate model, sampling plan. This process is commonly referred to as design of experiments

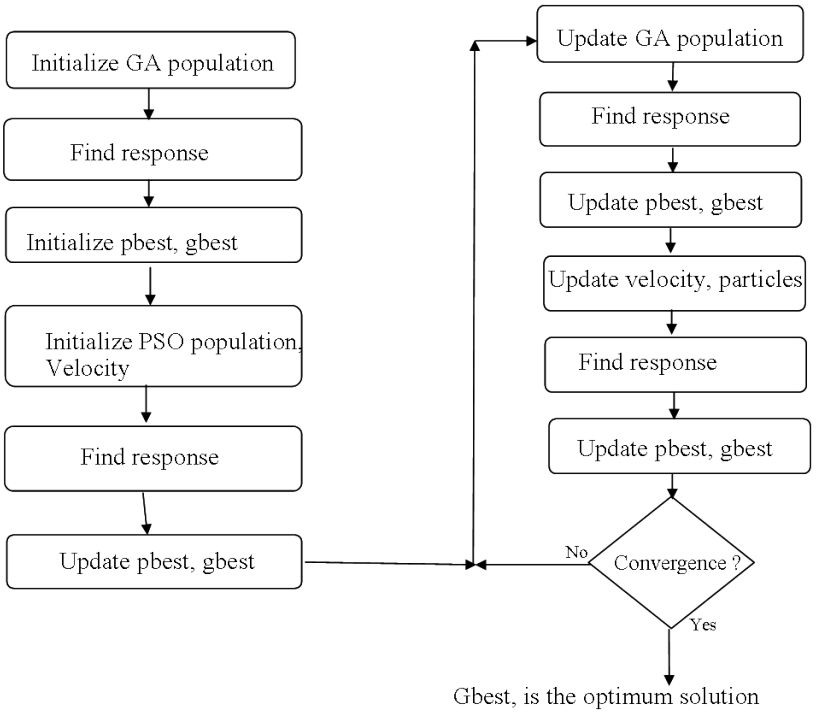

Figure 1. Hybrid GA-PSO optimization algorithm.

(DOE). This step is vital in building a surrogate model because the behavior of the response in the design space is unknown. The sampling plan selected should pick the design values distributed evenly throughout the entire design space. The sampling plan favored for initial surrogate model building is the space filling maximin, LHS technique. The sampling plan selected is also affected by the surrogate modeling technique being used.[?]

The LHS sampling points of k variables and n points are represented as $\mathbf{x}^{(i)} = \left(x_1^{(i)}, \cdots, x_k^{(i)}\right)$ and the associated function value is given by $y^{(i)} = y\left(\mathbf{x}^{(i)}\right)$, for $i = 1, \cdots, n$.

The simplest form of approximation is regression model is represented as:

$$y\left(x^{(i)}\right) = \sum_h \beta_h f_h\left(\mathbf{x}^{(i)}\right) + \epsilon^{(i)} \tag{1}$$

In this equation $f_h\left(\mathbf{x}^{(i)}\right)$, is a linear or nonlinear function of $\mathbf{x}$, β_h are unknowns and can be found using simple regression analysis. In this approximation $\epsilon^{(i)}$, the error term is assumed to be independent. However the response function is continuous and so the error which is a difference from the actual value to that of the approximated value is also continuous. This means that for any two points x_i and x_j close to each other the corresponding errors ϵ_i and ϵ_j are correlated. So the assumption that the error terms are independent is not correct and is more reasonable to assume that the errors are correlated. The correlation of errors at two sampling points $\mathbf{x}_i$ and $\mathbf{x}_j$ is given by,

$$Corr\left[\epsilon^{(i)}, \epsilon^{(j)}\right] = \exp\left[-d\left(\mathbf{x}^{(i)}, \mathbf{x}^{(j)}\right)\right] \tag{2}$$

where the distance, $d_{i,j}$ is calculated by the equation

$$d\left(\mathbf{x}^{(i)}, \mathbf{x}^{(j)}\right) = \sum_{h=1}^{k} \theta_h \left|x_h^{(i)} - x_h^{(j)}\right|^{p_h}, (\theta_h \geq 0, p_h \in [1, 2]) \tag{3}$$

In the above equation θ_h and p_h are the parameters for design and analysis of computer experiments (DACE). The variable θ_h can be interpreted as the measure of strength of the variable x_h. The exponent p_h is related to the smoothness of the correlation function.

The regression model can be expressed as

$$y\left(\mathbf{x}^{(i)}\right) = \mu + \epsilon^{\left(\mathbf{x}^{(i)}\right)} \tag{4}$$

Where μ is the mean of the response values.

The stochastic model has $2k+2$ parameters, $\mu, \sigma^2, \theta_1, \cdots, \theta_k, and p_1, \cdots, p_k$. These DACE parameters are estimated by maximizing the likelihood of the data sample selected.

The likelihood function is represented as

$$\frac{1}{(2\pi)^{n/2}\left(\sigma^2\right)^{n/2}|\mathbf{R}|^{1/2}} \exp\left[-\frac{(y-\mathbf{1}\mu)' R^{-1}(y-\mathbf{1}\mu)}{2\sigma^2}\right] \tag{5}$$

Given the correlation parameters θ_h and p_h we can solve for μ and σ^2 which can be used to find the likelihood function. By maximizing the likelihood function the DACE parameters θ_h and p_h as well as the mean and variance μ and σ^2 can be estimated.

The mean and variance are expressed as:

$\mu = \frac{\mathbf{1}'\mathbf{R}^{-1}y}{\mathbf{1}'\mathbf{R}^{-1}\mathbf{1}}$ and $\sigma^2 = \frac{(y-\mathbf{1}\mu)'R^{-1}(y-\mathbf{1}\mu)}{2\sigma^2}$

The response surface equation can be expressed as

$$y\left(\mathbf{x}^{(*)}\right) = \mu + \mathbf{r}'\mathbf{R}^{-1}(y-\mathbf{1}\mu) \tag{6}$$

where $\mathbf{r}'$ is the error correlation vector from the sampling point $\mathbf{x}^*$ to the points in the LHS table used to create the response surface. At any given sampling point in the LHS table the above equation reduces to the response value $y\left(x^{(*)}\right) = y^{(i)}$) thereby making the error at the LHS sampling points equal to zero.

The correlation of errors also effects our prediction accuracy. Intuitively, if the new sampling point $\mathbf{x}^*$ is close to $\mathbf{x}^i$, we should be more confident since they are highly correlated. The general mean squared error of the predictor can be denoted as

$$s^2\left(x^{(*)}\right) = \sigma^2\left[1 - \mathbf{r}'\mathbf{R}^{-1}r + \frac{\left(1-\mathbf{1}'\mathbf{R}^{-1}\mathbf{r}\right)^2}{\mathbf{1}'\mathbf{R}^{-1}\mathbf{1}}\right] \tag{7}$$

Based upon this mean squared error at the sampling location, we can estimate the expected improvement value, which is expressed as

$$E\left[I\left(\mathbf{x}\right)\right] = \left(f_{min} - y\right)\Phi\left(\frac{f_{min}-y}{s}\right) + s\phi\left(\frac{f_{min}-y}{s}\right) \tag{8}$$

where $\phi(\cdot) and \Phi(\cdot)$ are standard normal density and distribution function. The measure of the EIV gives us the guidance on the accuracy of the predicted value and also how much improvement can be achieved by adding a sample point at this predicted location.

III. Shape Optimization algorithm

The selected optimization algorithm, hybrid GA-PSO algorithm, is combined with the surrogate modeling technique in order to implement an efficient shape optimization process. The flow chart of the shape optimization algorithm is shown in figure 2. The initial training points for the response surface construction are selected using the LHS technique. Based upon our previous studies[9] we need at least 10 sampling points for each design variable to construct a initial response surface that captures all the trends in the given design space. The accuracy of the response surface is checked after every generation by using the measure of EIV. The confidence bound is set to 3% initially and is tightened to 2% to show the impact of the tighter bounds on the optimum shape.

III.A. Geometry of 2-D train nose

To demonstrate the proposed method a 2-dimensional shape of train was selected. Five control variables were selected to define the geometry of the train nose effectively. The shape of the nose considered is of the

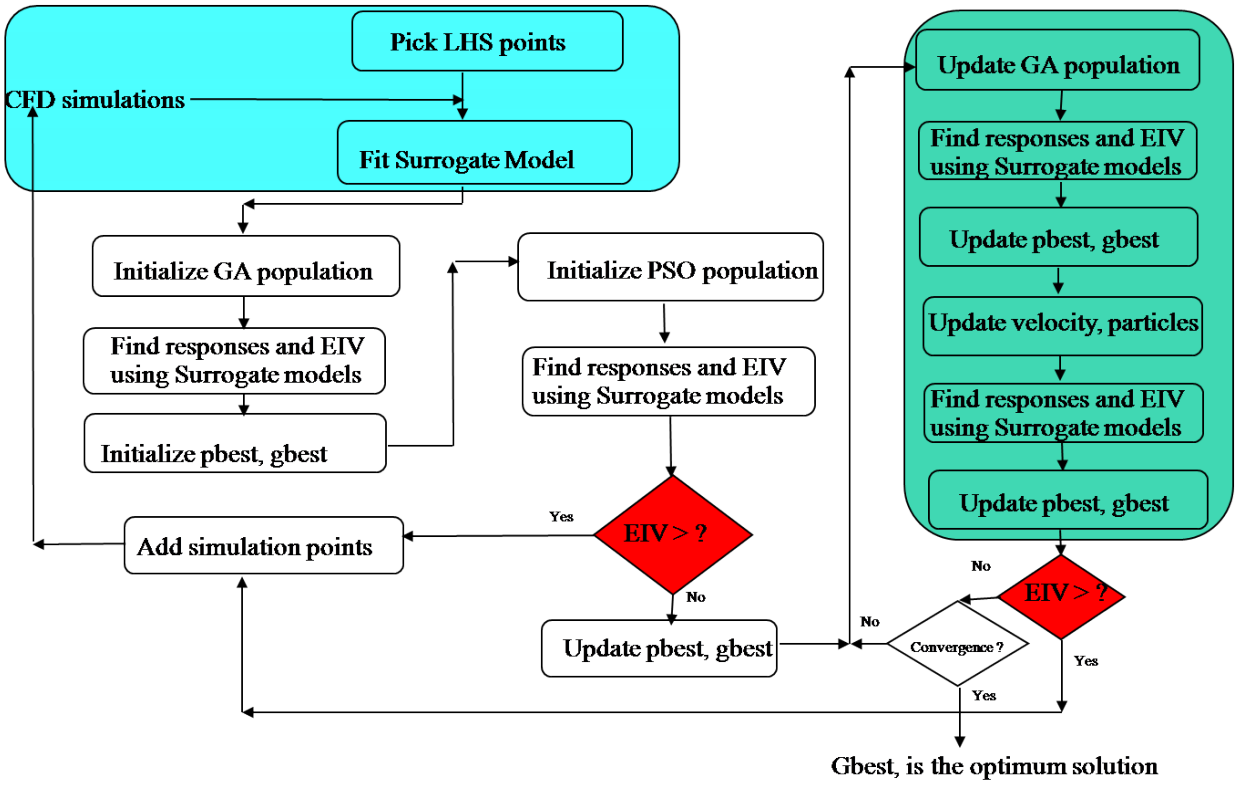

Figure 2. Flow chart showing the optimization process.

form of an ellipse. There are two length parameters which control the lengths of the top and the bottom ellipses, a height parameter to control the height of the nose, and two angle parameters that controls the sharpness of the nose. The 2-D geometrical parameters of the train are shown in Figure 3.

It is important to consider both the front and rear ends of the train to calculate the induced drag, therefore, the computational model includes both the front and back ends. To simplify and reduce the number of design variables it is assumed that the train is symmetrical along the center i.e. the front and the rear ends of the nose are identical. The train geometry also involves the middle section between the identical front and the back nose sections as shown in Figure 4 and the height of the train is assumed to be fixed as 4m. A gap of 0.4 m is modeled to consider the effect of the wheels and the flow under the train. CFD calculations are performed using CFD software SC/Tetra. A Pseudo 2-D unstructured mesh was generated with prism layers around the train to capture the boundary layer effects. A transient flow simulation is performed using unsteady RANS with $k-\epsilon$ with standard wall functions. Aerodynamic noise generated can be calculated by using the Lighthill equations.[10] Aerodynamic noise is predicted at the sampling points using acoustic analogy model in SC/Tetra. To observe the aerodynamic noise using the acoustic analogy, seven sample points were selected around the train body, three points on the front, three points in the rear end and one located at the center of the train and sound pressure levels were recorded for further analysis. The recorded aerodynamic pressure is converted into SPL using a fast Fourier transformation. The total computational mesh has around 300,000 elements and the simulation takes about 2 hours on a Linux cluster using eight cores. Analysis is performed for a total time period of 5 seconds, and the induced drag force is averaged for the same time period. The speed of the train in simulation is considered as 350 Km/hr.

III.B. Problem Setup

The objective functions are to minimize the induced drag and to minimize the aerodynamic noise generated because of the flow over the train.

$$min.F_d \tag{9}$$

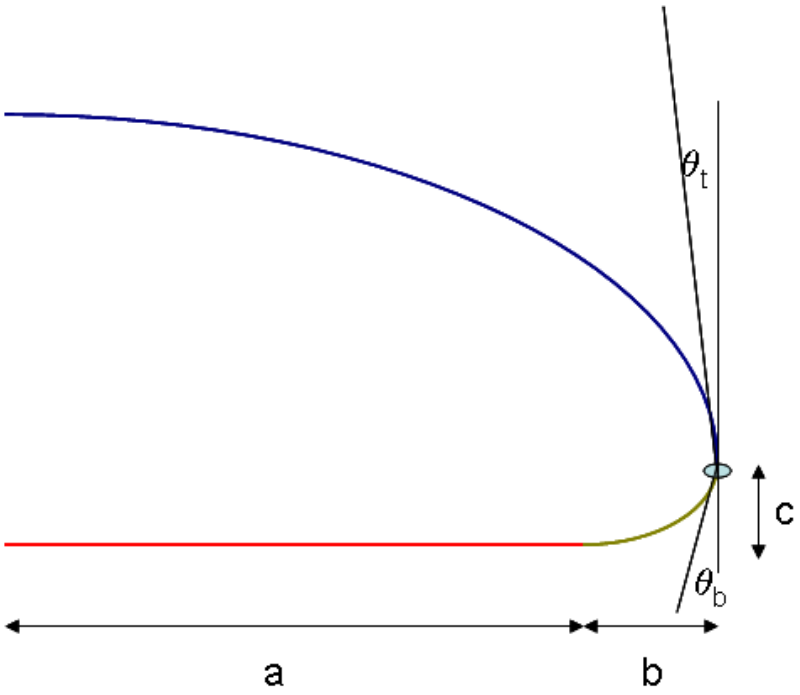

Figure 3. Geometric parameters of train nose.

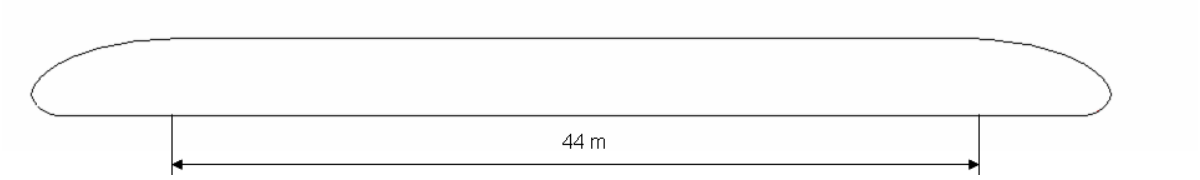

Figure 4. Geometry of the train with symmetric front and back sections.

and

$$min.F_S \tag{10}$$

Subjected to the geometry constraints

$$6.0 <= a <= 7.25 \tag{11}$$

$$1.25 <= b <= 2.75 \tag{12}$$

$$0.75 <= c <= 1.25 \tag{13}$$

$$0 <= \theta_b <= 20 \tag{14}$$

$$0 <= \theta_t <= 50 \tag{15}$$

IV. Results

The training points required to construct the surrogate model are selected using LHS technique. A total of 55 training points are selected to construct the initial surrogate model. The optimization algorithm has the capability to check the accuracy of the surrogate model by comparing the value EIV, and request for additional training points when ever necessary. For 3% confidence bounds the algorithm requested an additional two sampling points to improve the accuracy of the surrogate model. The confidence bound of 3% is satisfied using total training points of 57. There are two objectives in this optimization problem, minimize drag and minimize aerodynamic noise. Based upon the behavior of these response values, optimization problems with more than one objective function has more than one optimum solution.

A typical function value for optimization problems involving more than one objective functions is given by

$$f = \frac{w_1 f_1 + w_2 f_2}{w_1 + w_2} \tag{16}$$

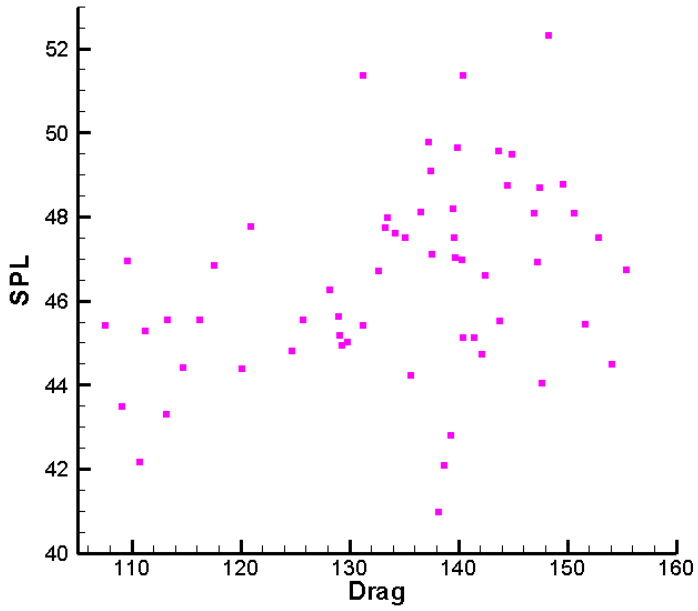

Figure 5. Drag Vs SPL for all the training points

The comparison of both the function values for the training points is shown in Figure 5. For this figure it is hard to fit a pareto curve since we don't have enough sampling points to fit an exact curve, which is commonly referred as the Pareto front.[11] All the solutions that fall on this Pareto front are the optimal values based upon the importance we put on each of the objectives.

The selection of the weights for the objective functions will have a significant effect on the final optimum shape, Since the weights will decide where the optimum falls on the pareto front. Optimization is performed using different weights ranging from 100% drag to 100% noise consideration. The optimization history with an objective function with 100% drag is shown in figure 6. Since the objective is to reduce only the drag, the optimization history shows the reduction of drag, the noise history shown is just the predicted value for that particular shape. It can be observed that the noise level increased during most of the optimization process thereby making these two functions contradicting each other. The optimum shape induces a drag force of 106.37 N and generates around 44.27 db of aerodynamic noise. The optimization history with the objective function to minimize only aerodynamic noise, combined objective function with 100% noise, is shown in figure 7. This resulted in an optimum shape that induces a drag force of 138.32 N and aerodynamic noise around 40.92 db. The optimization history confirms our observation that the objectives are contradicting each other and the optimum shape depends on the weights selected for each objective. Results for different combinations of weights are discussed now. The optimization history for a combined objective function with 80%drag and 20% noise is shown in figure 8. Resulting optimum shape induces a drag force of 106.37 N and generates aerodynamic noise of around 44.29 db. The optimization history with the combined objective function of 50%drag and 50% noise is showed in figure 9. This results in an optimum shape that induces a drag force of 109 N and the aerodynamic noise around 42.64 db. The optimization history with the combined objective function of 20%drag and 80% noise is showed in figure 10. The resulting optimum shape induces a drag force of 110.42 N and aerodynamic noise around 42.26 db.

The optimum shape parameters for different weights are shown in table 1. From these results it is evident that with the increase in the weight of aerodynamic noise in the objective function there is a slight increase in the induced drag along with the drop the aerodynamic noise. It can also be observed the length of the train

increases along with the increase of the weight on the aerodynamic noise. Using the data presented in table 1, the best weights to choose would be 50%, since we get a reduction of 2 db (around 5%)of aerodynamic noise for a slight increase (less than 3%) in the aerodynamic drag induced. The optimum nose shapes are shown in figure 11. It can also be observed that the nose shape has two distinct features. The nose shape is shorter and more pointed when the objective is to reduce drag. However, the nose length is longer and blunt when the objective is to reduce aerodynamic noise. These results were based on a confidence bound of 3% on the EIV.

The bounds are tightened, and reduced to an EIV of 2% to make the surrogate model more accurate. This required an addition of one more training point. The results from the optimization are presented in the table 2. The optimum nose shapes for different weights are shown in figure 12. The optimum shapes are shifted marginally compared to the 3% EIV results. However, the trend that the nose should be short and pointed to get the best drag performance and the nose should be long and blunt to get the least aerodynamic noise is maintained. The suggested method when compared against the results presented by Lorriaux,[12] took fewer number of function evaluations (CFD simulations) to find the optimum value, 180 against 57. The limitation of using GA as observed by Lorriaux, was that the results are initial population dependent and are not always repeatable. The results produced from the suggest method are repeatable and it takes a few seconds to repeat the optimization process once the response surface is created.

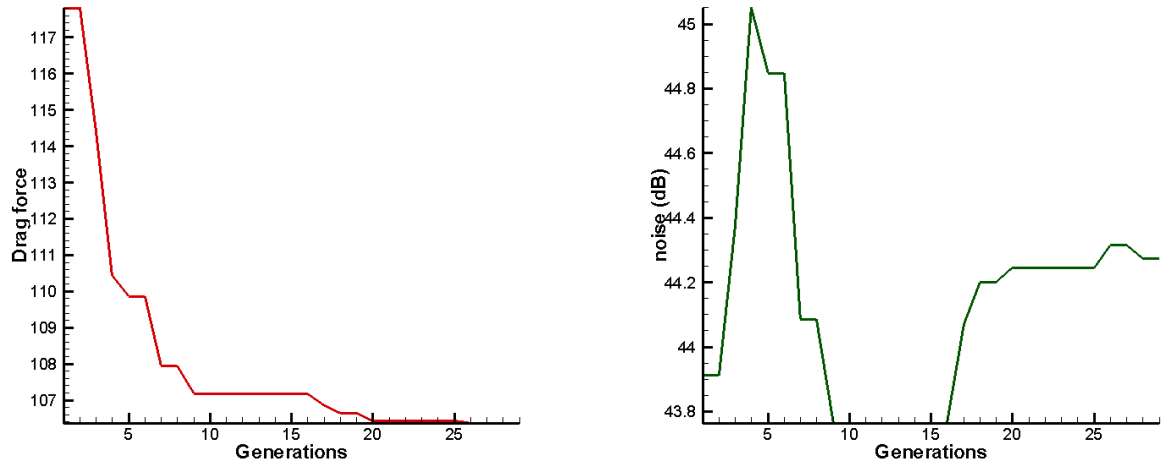

(a) Drag history (b) Noise history

Figure 6. Optimization history, 100% drag, 3% EIV

Table 1. Best shapes with 3% confidence bounds on EIV

W_d	W_a	a	b	c	θ_b	θ_t	Drag	Noise
1.0	0.0	6.756	1.350	0.796	13.5	46.4	106.37	44.27
0.8	0.2	6.774	1.368	0.796	15.5	47.2	106.37	44.29
0.5	0.5	6.841	1.632	0.824	14.9	47.7	109.07	42.64
0.2	0.8	6.919	1.654	0.808	14.9	46.98	110.42	42.26
0.0	1.0	7.089	1.611	1.157	16.6	29.6	138.32	40.93

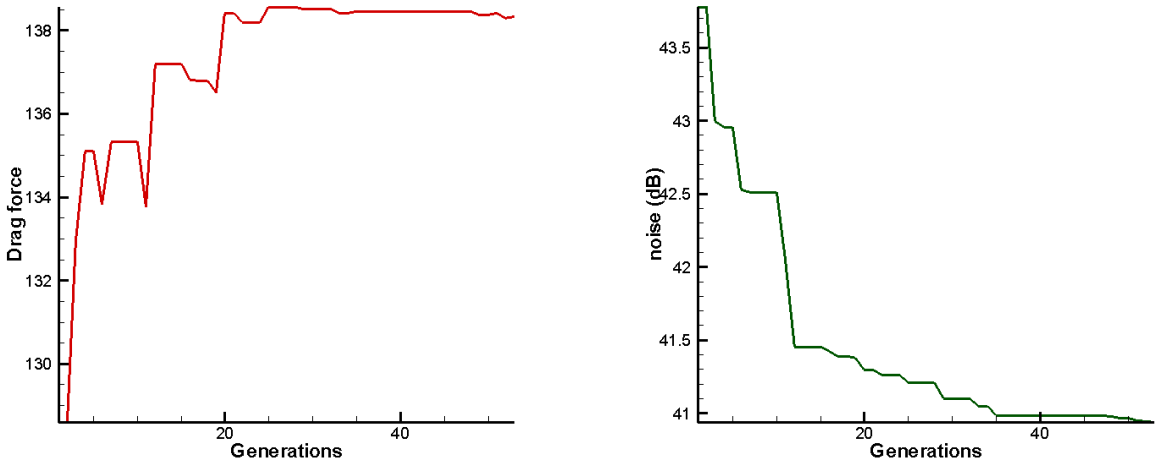

(a) Drag history (b) Noise history

Figure 7. Optimization history, 100% noise, 3% EIV

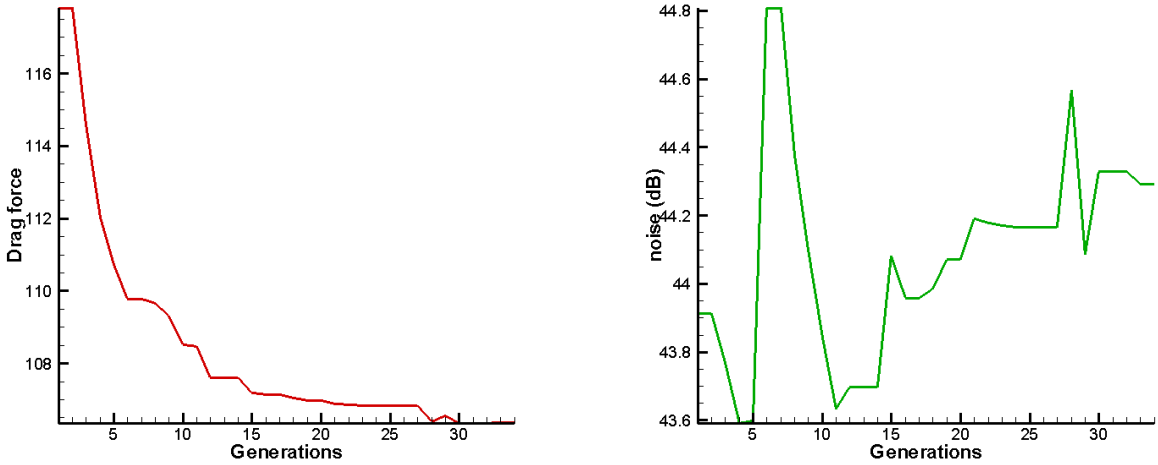

(a) Drag history (b) Noise history

Figure 8. Optimization history, 80% drag and 20% noise, 3% EIV

Table 2. Best shapes with 2% confidence bounds on EIV

W_d	W_a	a	b	c	θ_b	θ_t	Drag	Noise
1.0	0.0	6.715	1.333	0.788	17	47.2	106.65	45.29
0.8	0.2	6.783	1.625	0.795	16.7	47.28	108.2	43.23
0.5	0.5	6.843	1.655	0.789	14.7	47.3	108.8	42.5
0.2	0.8	6.917	1.654	0.801	15.0	47.0	110.03	42.3
0.0	1.0	7.000	1.612	1.160	16.6	29.6	138.5	41.03

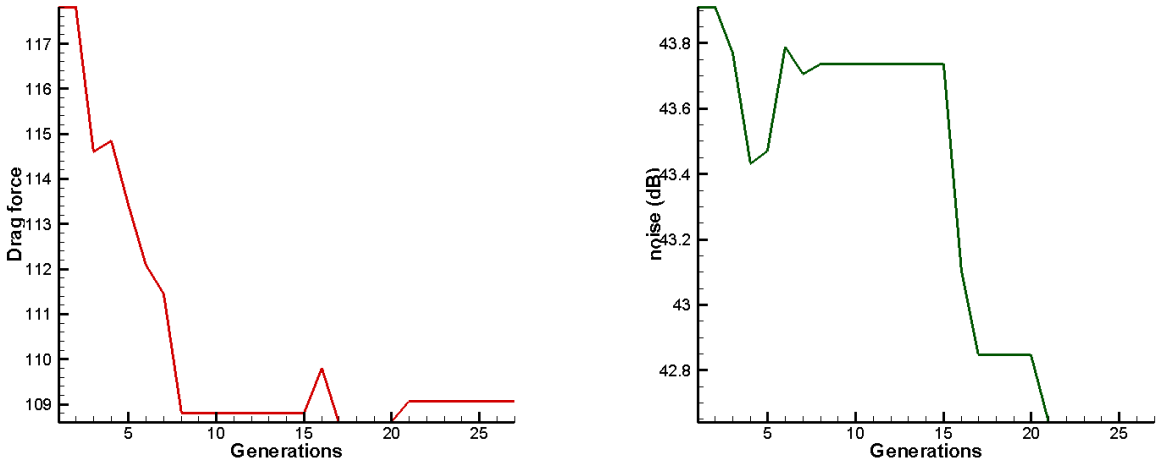

(a) Drag history (b) Noise history

Figure 9. Optimization history, 50% drag and 50% noise, 3% EIV

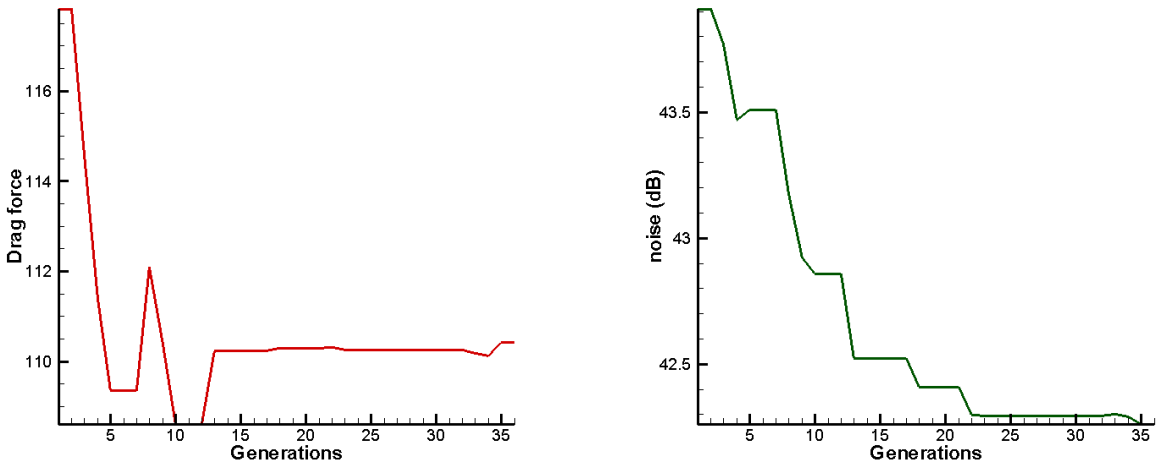

(a) Drag history (b) Noise history

Figure 10. Optimization history, 20% drag and 80% noise, 3% EIV

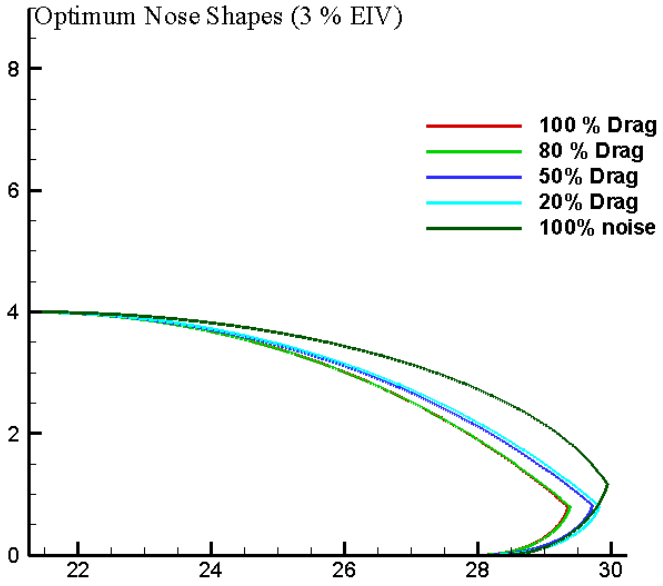

Figure 11. Optimum nose shapes with 3% Bounds on EIV .

V. Conclusions

Multi Objective Aerodynamic shape optimization of high speed train nose considering two objectives, minimizing aerodynamic drag and minimizing aerodynamic noise, was performed using a hybrid GAPSO algorithm. The feasibility of optimizing using a surrogate model in combination with a hybrid optimization algorithm is demonstrated successfully. It was observed that, around 11 LHS design points for each of the design variable are required to calculate the initial response surface that represents the behavior of the response. The test problem presented in this paper required two additional simulations for 3% confidence bounds. For a slightly tighter tolerances 2% confidence bounds required the addition of one more training points to improve the accuracy of the surrogate model. The effect of the choice of different weights on the optimum nose shape is studied. It was observed that the optimum shape that induces the least drag resulted in a nose shape which is slightly short and a pointed, where as the optimum shape that generates least aerodynamic noise was observed to be slightly long and bit more blunt. The best compromise would be to choose 50 % weights for both drag as well as noise. This results in a marginal drag increases by 2% but results in 6% reduction in the generated aerodynamic noise.

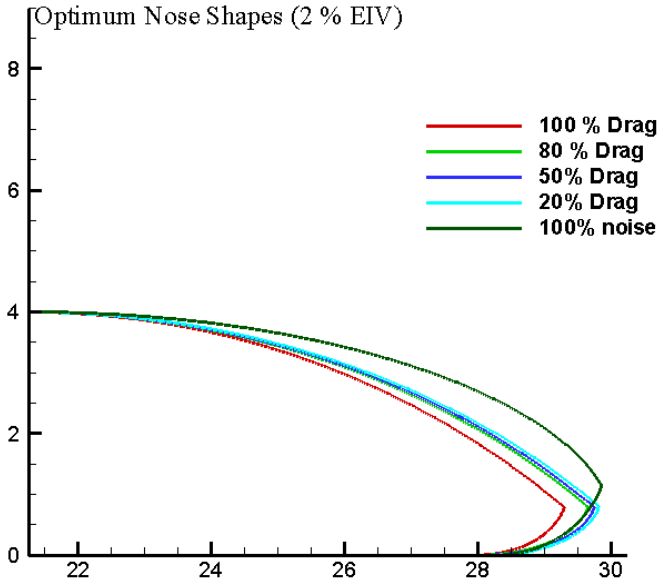

Figure 12. Optimum nose shapes with 2% Bounds on EIV .

References

[1]Raghu S. Raghunathan, H.-D. K. and Setoguchi, T., "Aerodynamics of high speed railway train," *Progress in Aerospace Sciences*, Vol. 38, 2002, pp. 469–514.

[2]Keane, A. J. and Scanlan, J. P., "Design earch and optimization in aerospace engineering," *Phil. Trans. R. Soc. A*, Vol. 365, 2007, pp. 2501–2529.

[3]Alexander I. J. Forrester, N. W. B. and Keane, A. J., "Optimization using surrogate models and partially converged computational fluid dynamics simulations," *Phil. Trans. R. Soc. A*, Vol. 462, 2006, pp. 2177–2204.

[4]Donald R. Jones, M. S. and Welch, W. J., "Efficient Global Optimization of Expensive Black-Box Functions," *Journal of Global Optimization*, Vol. 13, 1998, pp. 455–492.

[5]Barron J. Bichon, S. M. and Eldred, M. S., "Reliability-Based Design Optimization using Efficient Global Reliability Analysis," *50th AIAA/ASME/ASCE/AHS/ASC Structures Structural Dynamics and Materials Conference*, May 2009.

[6]Huang, L., Huang P., G., LeBeau Jr. P., R., and Hauser, T., "Optimization of Blowing and Suction Control on NACA 0012 Airfoil Using EARND Genetic Algorithm with Diversity Control," *Journal of Aircraft*, Vol. 44, 2007, pp. 1337–1349.

[7]Mathew, S. and Terence., S., "Breeding Swarms: A GA/PSO Hybrid," 2005.

[8]Kao, Y.-T. and Zahara, E., "A hybrid genetic algorithm and particle swarm optimization for multimodal functions," *Applied soft computing*, Vol. 8, 2009, pp. 849–857.

[9]Vytla V. V., Huang P., G. and Penmetsa, R. C., "Aerodynamic Shape Optimization of High Speed Train Nose using Surrogate Models," *48th AIAA Aerospace space sciences meeting including the new horizons forum and Aerospace Exposition*, 2010.

[10]Lighthill, M. J., "On Sound Generated Aerodynamically. I. General Theory," *Proceedings of the Royal Society of London. Series A, Mathematical and Physical Sciences*, Vol. 211, No. 107, 1952, pp. 564–587.

[11]Alba, E., Blum, C., Isasi, P., Leon, C., and Gomez, J. A., *Optimization Techniques for Solving Complex Problems*, Wiley series on parallel and distributed computing, 2009.

[12]Lorriaux E., B. N. and F., M., "Aerodynamic optimization of railway motor coaches," *http://webhost.ua.ac.be/eume/workshops/reallife/lorriaux.pdf* .